doi:10.1111/evo.13702

Shared extremes by ectotherms and endotherms: Body elongation in mustelids is associated with small size and reduced limbs

Chris J. Law,[1,2] Graham J. Slater,[3] and Rita S. Mehta[1]

[1]*Department of Ecology and Evolutionary Biology, Coastal Biology Building, University of California, Santa Cruz, California 95060*

[2]*E-mail: cjlaw@ucsc.edu*

[3]*Department of the Geophysical Sciences, University of Chicago, Chicago, Illinois 60637*

Received July 16, 2018
Accepted February 15, 2019

An elongate body with reduced or absent limbs has evolved independently in many ectothermic vertebrate lineages. While much effort has been spent examining the morphological pathways to elongation in these clades, quantitative investigations into the evolution of elongation in endothermic clades are lacking. We quantified body shape in 61 musteloid mammals (red panda, skunks, raccoons, and weasels) using the head-body elongation ratio. We also examined the morphological changes that may underlie the evolution toward more extreme body plans. We found that a mustelid clade comprised of the subfamilies Helictidinae, Guloninae, Ictonychinae, Mustelinae, and Lutrinae exhibited an evolutionary transition toward more elongate bodies. Furthermore, we discovered that elongation of the body is associated with the evolution of other key traits such as a reduction in body size and a reduction in forelimb length but not hindlimb length. This relationship between body elongation and forelimb length has not previously been quantitatively established for mammals but is consistent with trends exhibited by ectothermic vertebrates and suggests a common pattern of trait covariance associated with body shape evolution. This study provides the framework for documenting body shapes across a wider range of mammalian clades to better understand the morphological changes influencing shape disparity across all vertebrates.

KEY WORDS: **Body shape, Carnivora, evolutionary shifts, morphological innovation, Musteloidea, thoracolumbar vertebrae.**

As one of the most prominent axes of phenotypic variation among vertebrates, body shape plays a prominent role in determining niche specialization and may push the boundaries of morphological, functional, and ecological evolution within a clade (Gans 1975; Wiens et al. 2006; Claverie and Wainwright 2014; Sharpe et al. 2015; Collar et al. 2016). Recent quantitative comparative studies have led to an improved understanding of the morphological underpinnings of extreme body shapes in vertebrates and their contributions to body shape diversity (Gans 1975; Wiens et al. 2006; Claverie and Wainwright 2014; Sharpe et al. 2015; Collar et al. 2016). These studies emphasize that body shape is a multivariate trait that varies along two major axes, from short-bodied to long-bodied and from deep- or wide-bodied to skinny-bodied (Bergmann and Irschick 2012; Collar et al. 2013; Claverie and Wainwright 2014). The limbs, or lack thereof, also contribute to the disparity in body shapes.

Elongation is the dominant axis of shape diversification in squamate reptiles (Bergmann and Irschick 2012) and teleost fishes (Claverie and Wainwright 2014) and, at its extreme, results in eel- or snake-like forms. Body elongation facilitates diverse behaviors, particularly related to locomotion (Webb 1982; Brainerd and Patek 1998; Bergmann and Irschick 2009) and foraging (Gans 1983; Mehta and Wainwright 2007; Mehta et al. 2010). For example, body elongation in moray eels and snakes has led to novel behaviors such as knotting, rotation, constriction, and striking reaches necessary to capture and consume large prey items (Miller 1989; Cundall and Greene 2000; Mehta et al. 2010; Lillywhite

2014; Diluzio et al. 2017). Associated with this phenotype is structural reduction or loss of the limbs (Gans 1975). Despite observed convergence in extreme phenotypes, the mechanisms underlying elongation in vertebrates vary; increases in body elongation across evolutionary time can occur through multiple pathways such as reduction of body depth or width, elongation of the head, and/or extension of body length by increasing the length of individual vertebrae (Parra-Olea and Wake 2001; Ward and Brainerd 2007; Ward and Mehta 2010; Collar et al. 2013). Elongate body plans also commonly arise through increases in the number of vertebrae in a particular region of the axial skeleton (Richardson et al. 1998; Polly et al. 2001; Ward and Brainerd 2007; Ward and Mehta 2010; Mehta et al. 2010).

Studies of body shapes in mammals have somewhat lagged behind those of ectotherms. This discrepancy may not be surprising as elongate bodies are less common in mammals, and the extremely elongate bodies observed in eels and snakes are nonexistent. Infrequent examples of elongation in mammals are thought to be related to the greater metabolic challenge imposed by an increased surface-to-volume ratio in homeotherms (Scholander et al. 1950; Brown et al. 1972; Lindstedt and Boyce 1985). Differential patterning in vertebral number may also play a role, as almost all mammal lineages exhibit only seven cervical vertebrae, 19–20 thoracolumbar vertebrae, and 2–5 sacral vertebrae (Narita and Kuratani 2005). This numerical precision in precaudal vertebral number drastically contrasts with the 100–450 vertebrae present in some snakes (Polly et al. 2001; Ward and Mehta 2014). Despite the striking lower vertebral number in mammals, heterochronic pathways during somitogenesis have resulted in considerable changes in vertebral shapes, generating diverse body plans from long-necked giraffes to tiny mice (Buchholtz 2001; Buchholtz and Schur 2004; Arnold et al. 2017). Where distinct shape transitions exist and functional consequences are apparent, biomechanical studies have investigated the relationships between maximum length and maximum body thickness (fineness ratio) in aquatic and semi-aquatic mammals and their impact on streamlining during swimming (Fish 1993; Fish et al. 2008). In terrestrial mammals, much work has focused on the diversity found in the cervical region (Hautier and Weisbecker 2010; Varela-Lasheras et al. 2011; Buchholtz 2014; Arnold et al. 2017). Although the thoracolumbar region plays a critical role in locomotion (Kardong 2014), few researchers have quantitatively tested hypotheses pertaining to the evolution and diversity of this region of the axial skeleton in mammals and its contribution toward defining body shape and species diversification.

In this study, we use the mammalian superfamily Musteloidea to examine the evolution of body shape, its underlying components, and the relationship with limb lengths. Musteloidea is comprised of four families: Mephitidae (skunks and stink badgers), Ailuridae (the red panda), Procyonidae (raccoons, coatis, olingos, and kinkajou), and Mustelidae (badgers, martens, minks, otters, polecats, and weasels). For centuries, mustelid carnivorans such as weasels, polecats, minks (subfamily Mustelinae), otters (subfamily Lutrinae), and martens (subfamily Guloninae) have been described as small and elongate (Shaw 1800; Griffith 1827; Gray 1865; Brown et al. 1972; Gliwicz 1988; King 1989; Zielinski 2000), but these qualitative observations are not supported by any rigorous quantification of body shape. The lack of quantitative data on mustelid body shape is unfortunate given that time-calibrated molecular phylogenetic studies have resulted in the hypothesis of a critical role for elongation in facilitating the diversification of mustelids during the Late Miocene (Koepfli et al. 2008; Sato et al. 2012; Law et al. 2018). The Late Miocene was characterized by arid climates (Zachos et al. 2008) and expansion of open grassland and woodland habitats (Edwards et al. 2010; Strömberg 2011), which in turn has been interpreted as facilitating an increase in small burrowing rodents and lagomorph diversity relative to early Miocene times (Finarelli and Badgley 2010; Fabre et al. 2012; Samuels and Hopkins 2017). Some authors (e.g., Baskin 1998; Koepfli et al. 2008; Sato et al. 2012) have suggested that small, elongate body plans may have enhanced the ability of mustelids to enter burrows and confined spaces to capture prey, as many extant species do (Brown et al. 1972; Gliwicz 1988; King 1989) and therefore played a role in promoting the spread and subsequent diversification of the clade. Recent quantitative tests of these hypotheses based on a phylogeny of extant musteloids and the musteloid fossil record provide no evidence of a pulse of increased speciation during this climate transition (Law et al. 2018). However, these authors did recover strong support for a scenario in which a subclade of putatively elongate mustelids (consisting of the subfamilies Helictidinae, Guloninae, Ictonychinae, Mustelinae, and Lutrinae; blue box in Fig. 1) exhibited decoupled diversification dynamics from the rest of the clade. In addition, analysis of rates of body length and mass evolution show that these two traits are also decoupled within this mustelid subclade (yellow-green box in Fig. 1), with the branches leading toward Ictonychinae, Mustelinae, and Lutrinae exhibiting an increase in the rate of body length evolution without an associated increase in the rate of body mass evolution. These patterns suggest that an association between elongation and diversification rates is worthy of further scrutiny.

We test the hypothesis that the clades Helictidinae, Guloninae, Ictonychinae, Mustelinae, and Lutrinae exhibit evolutionary transitions toward more elongate bodies. Because elongation of the body is a complex trait with multiple morphological pathways (Parra-Olea and Wake 2001; Ward and Brainerd 2007; Ward and Mehta 2010; Collar et al. 2013), we also identify the cranial and axial regions underlying body elongation and predict that multiple morphological components contribute to elongation of the body axis. Furthermore, as body elongation in ectotherms is associated

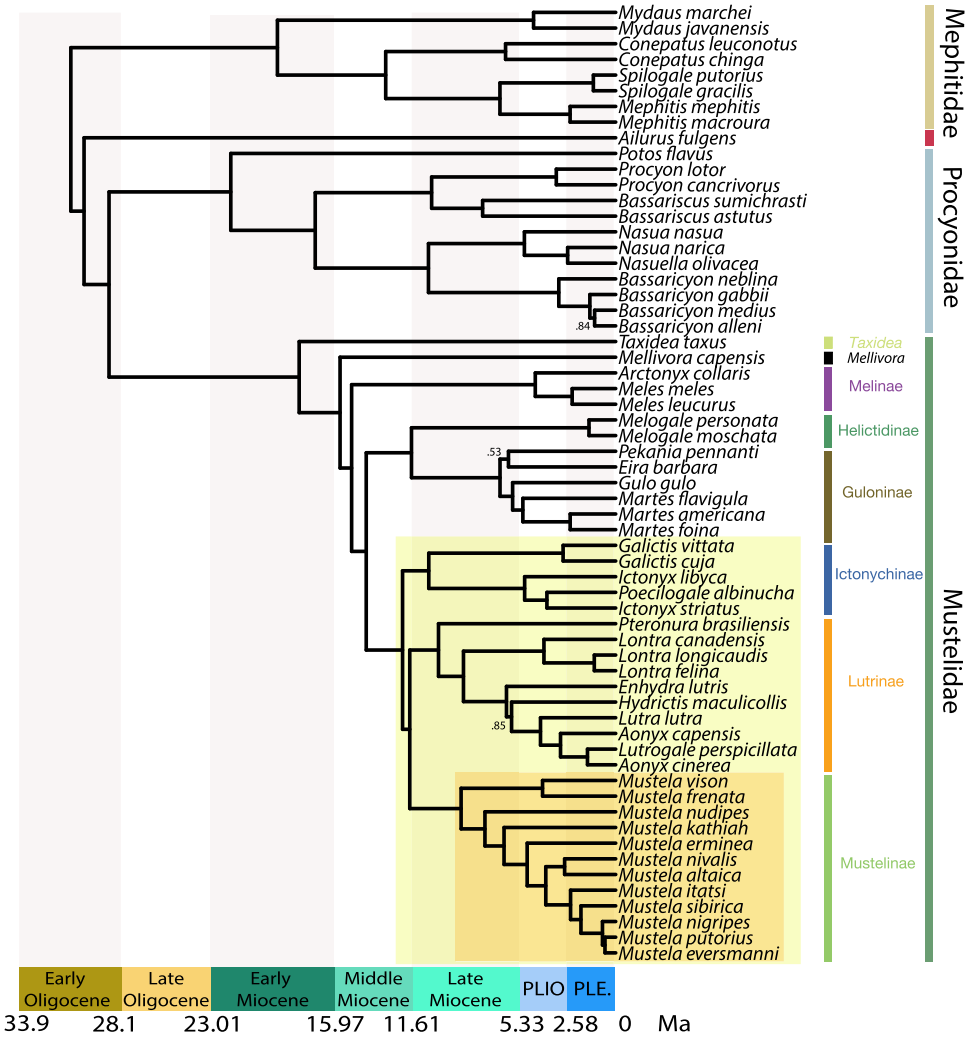

Figure 1. **Pruned time calibrated phylogeny of Musteloidea redrawn from Law et al. (2018). The shaded blue box indicates the mustelid subclade (subfamilies Helictidinae, Guloninae, Ictonychinae, Mustelinae, and Lutrinae) that exhibits higher clade carrying capacity relative to the rest of Musteloidea. The shaded yellow-green box indicates the mustelid subclade (Ictonychinae, Mustelinae, and Lutrinae) that exhibits an increase in the evolutionary rate of body length without an increase in the evolutionary rate of body mass. The shaded orange box highlights Mustelinae (weasels and polecats), the clade often considered the hallmark example of body elongation within Mustelidae. All nodes are supported by posterior probabilities > 0.95 except where noted. PLIO = Pleistocene; PLE = Pliocene.**

with a suite of complementary traits such as a reduction in size and shorter limbs, we also test for relationships between body size and body shape evolution across musteloids and ask whether more elongate body morphologies correspond with a reduction in limb lengths.

Methods

QUANTIFYING BODY SHAPE, SIZE, AND LIMB LENGTH

We quantified body shape, body size, and limb lengths using osteological specimens cataloged at the American Museum of Natural History, the California Academy of Sciences, the Field Museum, the Museum of Southwestern Biology, the Museum of Vertebrate Zoology, the National Museum of Natural History, and the Natural History Museum of Los Angeles County. Our dataset consisted of 61 musteloid species (roughly 72% of species-level diversity), sampling between one and ten individuals per species ($N = 277$ individuals; median $= 5$ individuals; $N \geq 4$ individuals for 40 species) spread across the major clades (Table S1). All specimens were fully mature, determined by the closure of exoccipital–basioccipital and basisphenoid–basioccipital sutures on the cranium and ossification of all vertebrae and limb bones. Specimens were a combination of females, males, and unknowns. Although many musteloids exhibit sexual dimorphism in the cranial and axial skeletons (Holmes and Powell 1994; Morris and Carrier 2016; Law and Mehta 2018), we were unable to use just one sex without

compromising sample sizes in both the number of species and the number of individuals per species used. We tried to maintain even sex ratios for our species averages when possible. Measurements were taken to the nearest 0.01 mm with digital calipers (see Table S1 for specimen list).

We quantified musteloid body shape by adopting a modular set of measurements for quantifying transitions in shape and their underlying morphological components (Collar et al. 2013). We calculated the head-body elongation ratio (ER) as the sum of head length (L_H) and body length (L_B) divided by the body depth (L_R): head-body $ER = \frac{L_H+L_B}{L_R}$. We measured head length as the condylobasal length of the cranium. We estimated body length by summing the centrum lengths (measured along the ventral surface of the vertebral centrum) of each cervical, thoracic, lumbar, and sacral vertebra, and we estimated body depth as the average length (measured from the end of the capitulum to the point of articulation with the costal cartilage) of the four longest ribs (Fig. 2). We omit measurements of the caudal region in our calculation of body length because the number of caudal vertebrae in most musteloid species is unknown and there was no way to determine whether the osteological specimens that we used contained all caudal vertebrae.

We also examined how the various regions of the cranial and axial skeletons contribute to body shape variation. We quantified head elongation ratio (head ER) by dividing cranial length (L_H) by cranial height (H_H). We then used a modified version of the axial elongation index (AEI) (Ward and Brainerd 2007) to examine how each vertebral region (i.e., cervical, thoracic, lumbar, and sacral) contributes to elongation. For each region (V), we calculated AEI_V as the total sum of vertebral lengths (L_V measured along the ventral surface of the vertebral centrum) divided by the average vertebral height (H_V measured from the ventral surface of the centrum to the tip of the neural spine): $AEI_V = \frac{\Sigma L_V}{mean(H_V)}$ (Fig. 2).

We quantified body size as the geometric mean of linear measurements taken from the cranium, vertebrae, and ribs (i.e., L_H, H_H, L_R, and ΣL_V and ΣH_V of vertebrae in each region). The geometric mean was derived from the Nth root of the product of N linear measurements, a widely used as a predictor of the size of an individual (Mosimann 1970; Jungers et al. 1995). Lastly, we measured the lengths of the forelimb and hindlimb (Fig. 2). Forelimb length was recorded as the sum of the humerus (measured from the dorsal point of the humeral head to the ventral point of the capitulum) and radius lengths (measured from the dorsal point of the radial head to the ventral point of the styloid process), and hindlimb length was recorded as the sum of the femur (measured from the dorsal point of the femoral neck to the ventral point of the patellar surface) and tibia lengths (measured from the dorsal point of the intercondylar eminence to the ventral point of the articular surface). All indices were plotted as box and whisker plots to examine variation in raw data between Mephitidae, Ailuridae, Procyonidae, and mustelid subfamilies (Fig. 3) and natural-log (ln) transformed prior to performing phylogenetic comparative analyses.

PHYLOGENY

We assessed the evolution of musteloid body shape and size using a phylogenetic comparative approach with a recently published musteloid phylogeny (Fig. 1; Law et al. 2018). This time-calibrated tree was inferred in a Bayesian framework using a supermatrix of 46 genes (four mitochondrial and 42 nuclear genes) from 75 of the 85 putative musteloid species (88.2% of musteloid species representing all 33 musteloid genera). We incorporated 74 phylogenetically constrained fossil musteloids to assist with divergence time estimation by using the fossilized birth-death (FBD) tree process prior (Heath et al. 2014) extended to allow for sampled ancestors (Gavryushkina et al. 2014).

PREDICTION 1: MUSTELIDS EXHIBIT MORE ELONGATE BODIES COMPARED TO OTHER MUSTELOIDS

To explicitly test hypotheses that clades within Mustelidae exhibit evolutionary transitions toward more elongate bodies, we fitted five macroevolutionary models to our head-body ER dataset using maximum likelihood (Hansen 1997; Butler and King 2004; Beaulieu et al. 2012). We first fit a single-rate Brownian motion model (BM1), which allows head-body ER evolution to proceed as a random walk and head-body ER variance to accumulate proportional to time, and single peak Ornstein–Uhlenbeck model (OU1), which constrains head-body ER to evolve about a single, stationary peak. Support for the BM1 model would suggest that variance in body shape is simply accumulating through evolutionary time, whereas support for the OU1 model would suggest that the entire musteloid clade is evolving toward a single body shape optimum. We then tested whether the central tendency for head-body ER (Θ) transitioned between a priori designated regimes (i.e., between putatively elongate musteloid species and the remaining musteloids) by fitting a series of two-peak OU (OUM) models. The strength of selection (α) and stochastic diffusion (σ^2) parameters were held constant across regimes because our low species sample size makes these parameters difficult to estimate and interpret (Beaulieu et al. 2012). Because previous work has demonstrated decoupled diversification dynamics and differential rates of body length and mass evolution within mustelid clades (Law et al. 2018), we fit two-peak OUM models under three distinct phylogenetic scenarios. The first model (OUM_A) tested for a transition in head-body ER between the mustelid subclade that exhibited increased clade carrying capacity (Helictidinae, Guloninae, Ictonychinae, Mustelinae, and Lutrinae; blue

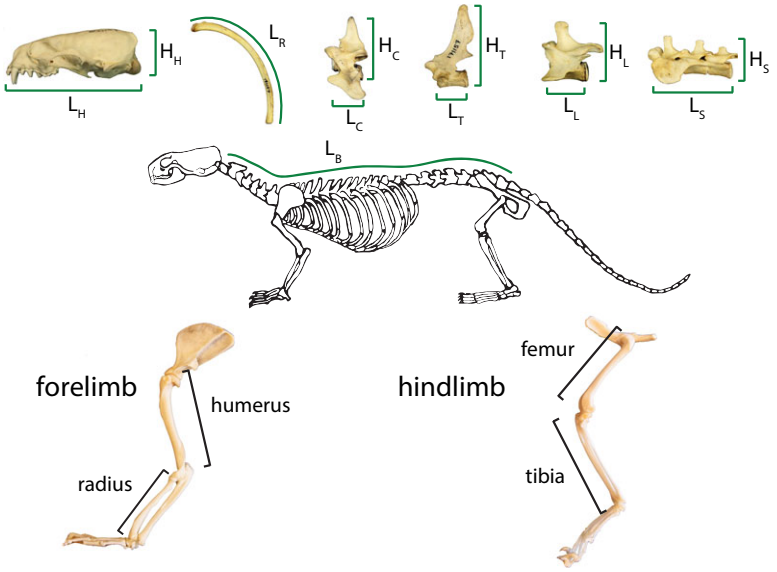

Figure 2. Measurements of body regions used to calculate head-body ER, head ER, and AEI of the cervical, thoracic, lumbar, and sacral regions. L_X = lengths and H_X = heights. See text for calculations. H = head; R = rib; C = cervical; T = thoracic; L = lumbar; S = sacral; B = body length. Forelimb length was recorded as the sum of the humerus (measured from the dorsal point of the humeral head to the ventral point of the capitulum) and radius lengths (measured from the dorsal point of the radial head to the ventral point of the styloid process), and hindlimb length was recorded as the sum of the femur (measured from the dorsal point of the femoral neck to the ventral point of the patellar surface) and tibia lengths (measured from the dorsal point of the intercondylar eminence to the ventral point of the articular surface).

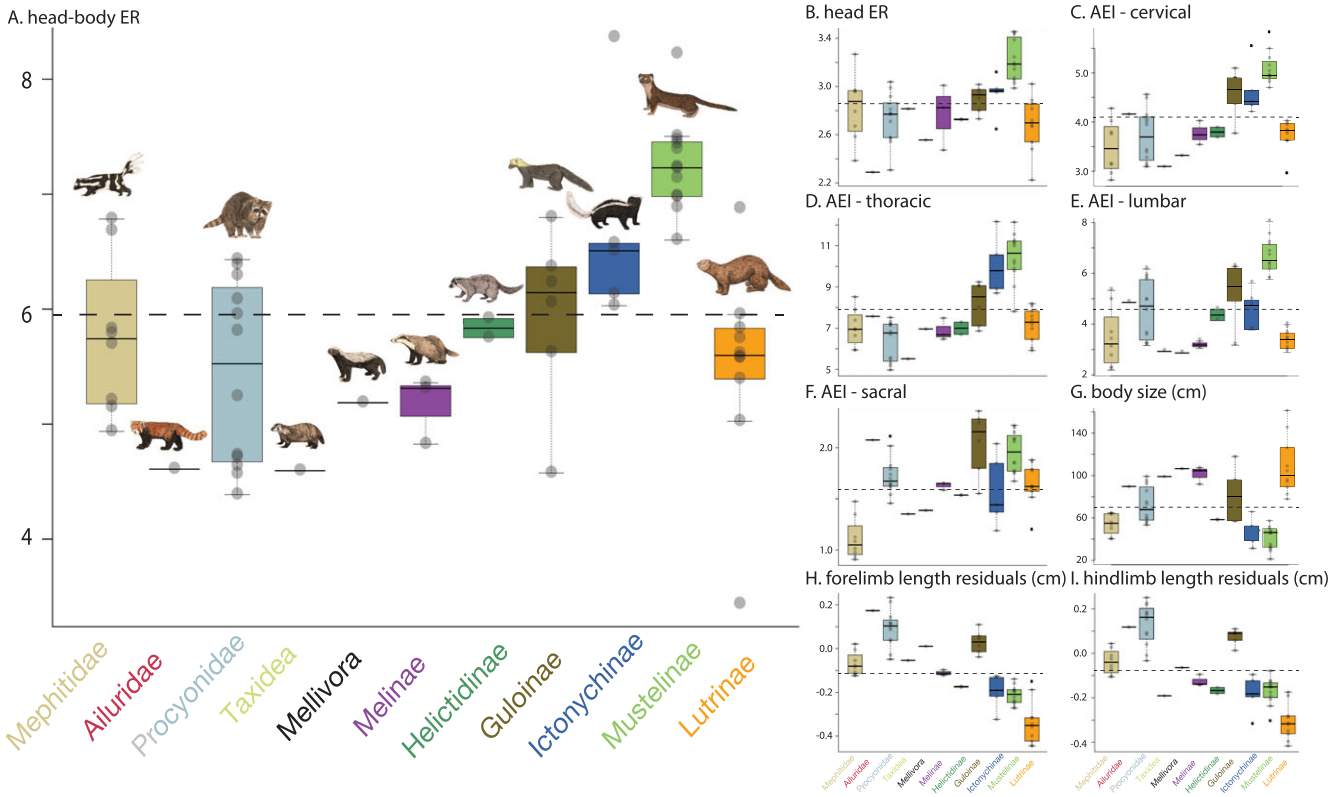

Figure 3. Box and whisker plots of head-body ER (A), head ER (B), cervical AEI (C), thoracic AEI (D), lumbar AEI (E), sacral AEI (F), body size (G), forelimb length (H), and hindlimb length (I), showing variation in raw data between Mephitidae, Ailuridae, Procyonidae, and mustelid subfamilies. Dashed black lines indicate mean value of each trait.

box in Fig. 1) and the remaining musteloids. The second model (OUM_B) tested for a transition in head-body ER between the mustelid subclade that exhibited decoupled evolutionary rates in body length and mass (Ictonychinae, Mustelinae, and Lutrinae; yellow-green box in Fig. 1) and the remaining musteloids. The third model (OUM_C) tested for a transition in head-body ER between a designated clade consisting of just musteline weasels and polecats (*Mustela* spp.; orange box in Fig. 1) and the remaining musteloids. This third model was tested because musteline weasels and polecats are considered the hallmark example of body elongation within Mustelidae (Brown et al. 1972; Gliwicz 1988; King 1989). All models were fit using the *OUwie* function in the R package OUwie (Beaulieu et al. 2012). The three designated elongate/nonelongate regimes were mapped onto the musteloid phylogeny using the paintSubTree function in phytools (Revell 2011). We accounted for measurement error of head-body ER by incorporating the standard errors of species means to each model. We used pooled sample standard error for samples with only one specimen. Relative support for each of the five models was assessed through computation of small sample corrected Akaike weights (AICcw). Lastly, we calculated the phylogenetic half-life of head-body ER as $\ln(2)/\alpha$.

We fit the same set of evolutionary models to head ER and AEI of cervical, thoracic, lumbar, and sacral independently to determine which morphological component(s) drive body shape evolution. Although the total number of thoracolumbar vertebrae is almost always fixed at 20 in musteloids, the proportion among the two regions can vary between species (13–16 thoracic vertebrae and 4–7 lumbar vertebrae). To account for this variation in vertebral number, we repeated the analyses using the average aspect ratio (ΣL_{TV} divided by ΣH_{TV}) of the thoracic vertebrae and the average aspect ratio (ΣL_{LV} divided by ΣH_{LV}) of the lumbar vertebrae. We also fit the same set of evolutionary models to body size and limb lengths. We used size-corrected fore- and hindlimb lengths by obtaining residuals from phylogenetic regression of each limb length dataset on the geometric mean of all our linear measurements with the phyl.resid function in the package phytools (Revell 2011). All natural-logged transformed optimal values were converted back to and reported as raw optimal values.

PREDICTION 2: TRANSITIONS IN BODY SHAPE ARE ACCOMPANIED BY TRANSITIONS IN BODY SIZE AND LIMB REDUCTION

The evolutionary pattern of increased body elongation with limb reduction is well documented in several clades of ectothermic vertebrates (Gans 1975; Wiens and Slingluff 2001; Brandley et al. 2008; Morinaga and Bergmann 2017). Whether this trend is also found in mammals is not known. Therefore, we examined the relationship between body shape (head-body ER) and limb lengths as well as the relationship between body shape and body size (geometric mean) using phylogenetic generalized least-squares (PGLS) regressions so that these patterns can be directly compared to ectothermic vertebrates. Because there is a negative relationship between body size and head-body ER (see Results), we used size-corrected head-body ER and size-corrected limb lengths obtained from residuals extracted for each trait against the geometric mean. All regression parameters were simultaneously estimated with phylogenetic signal in the residual error as Pagel's lambda (Pagel 1999; Revell 2010) using the phylolm function in the R package phylolm (Tung Ho and Ané 2014). All analyses were performed in R 3.3 (R Core Team 2017).

Results

PREDICTION 1: MUSTELIDS EXHIBIT MORE ELONGATE BODIES COMPARED TO OTHER MUSTELOIDS

Musteloids exhibit great variation in head-body ER (Fig. 3). We found that the three 2-peak OUM models were the best-fitting models (combined AICcW > 0.75) for the evolution of body shape using head-body ER. There was greatest support (AICcW $=$ 0.44) for the 2-peak OUM_A model in which a mustelid subclade consisting of Helictidinae, Guloninae, Ictonychinae, Mustelinae, and Lutrinae evolved toward a higher head-body ER optimum ($\Theta_{mustelid} = 6.97$) compared to the rest of the musteloid clade ($\Theta_A = 5.25$). The alpha parameter for this model (0.06 myr^{-1}) corresponds to a phylogenetic half-life (11.19 myr) that is close to the age of the subclade itself (14.84 myr). This long half-life indicates that helictidines, gulonines, ictonychines, mustelines, and lutrines are slowly evolving toward a more elongate body optimum. Although the phylogenetic means of these mustelid subclades differ substantially from the ancestral state of Musteloidea, phylogenetic signal ($\lambda = 1.01$; $P < 0.001$) in head-body ER is too high for the subclade to be evolving under an OU-like process. To corroborate this, we fit the BMS model of Thomas et al. (2006), which allows for distinct phylogenetic means without invoking a strength of selection parameter, to our three elongate subclade designations (BMS_A, BMS_B, and BMS_C, respectively). The stronger support for the BMS_A model over an OUM model in head-body ER (AICcW $= 0.56$; Table 1) confirms that constrained evolution is not required to explain the shift in head-body ER and that rapid evolution along the branch leading to the clade consisting of Helictidinae, Guloninae, Ictonychinae, Mustelinae, and Lutrinae with a subsequent return to BM-like dynamics in the crown group is sufficient to explain the trait data. We confirmed that false-positive rates (i.e., the rate at which single-regime BM data are erroneously identified as BMS-like) for this test were

Table 1. Parameter estimates and model fits of (A) head-body ER, (B) head ER, and AEI of the (C) cervical, (D) thoracic, (E) lumbar, and (F) sacral regions.

A. head-body ER

Model	α	ln(2)/α	σ^2	Θ_A	Θ	lnL	*k*	AICc	ΔAICc	AICcW
BM1	NA	–	0.00	5.32	–	36.90	2	−69.59	6.23	0.02
OU1	0.04	16.89	0.00	5.43	–	37.98	3	−69.54	6.28	0.02
OUM_A	0.06	11.19	0.00	5.25	6.97	40.43	4	−72.14	3.67	0.09
OUM_B	0.06	10.69	0.00	5.37	6.99	39.43	4	−70.14	5.68	0.03
OUM_C	0.09	8.15	0.00	5.49	8.96	39.37	4	−70.03	5.79	0.03
BMS_A	**NA**	–	**0.00**	**5.19**	**8.06**	**42.27**	**4**	**−75.82**	**0.00**	**0.56**
BMS_B	NA	–	0.00	5.26	7.82	40.45	4	−72.18	3.64	0.09
BMS_C	NA	–	0.00	5.34	4.85	40.89	4	−73.07	2.75	0.14

B. head ER

Model	α	ln(2)/α	σ^2	Θ_A	Θ	lnL	*k*	AICc	ΔAICc	AICcW
BM1	NA	–	0.00	2.67	–	62.05	2	−119.90	11.83	0.00
OU1	0.07	9.62	0.00	2.74	–	64.49	3	−122.56	9.17	0.01
OUM_A	0.10	7.29	0.00	2.70	2.97	65.81	4	−122.91	8.82	0.01
OUM_B	0.09	7.41	0.00	2.73	3.00	65.39	4	−122.06	9.67	0.01
OUM_C	**0.57**	**1.22**	**0.01**	**2.76**	**3.24**	**70.22**	**4**	**−131.73**	**0.00**	**0.97**
BMS_A	NA	–	0.00	2.65	3.11	62.75	4	−116.79	14.93	0.00
BMS_B	NA	–	0.00	2.66	3.10	63.81	4	−118.90	12.83	0.00
BMS_C	NA	–	0.00	2.67	4.40	63.09	4	−117.46	14.26	0.00

C. AEI cervical

Model	α	ln(2)/α	σ^2	Θ_A	Θ	lnL	*k*	AICc	ΔAICc	AICcW
BM1	NA	–	0.00	3.66	–	48.79	2	−93.38	0.81	0.21
OU1	0.00	–	0.00	3.66	–	48.79	3	−91.16	3.03	0.07
OUM_A	0.02	39.76	0.00	3.56	5.33	51.32	4	−93.92	0.27	0.27
OUM_B	0.00	NA	0.00	3.64	4.50	49.20	4	−89.68	4.51	0.03
OUM_C	0.00	NA	0.00	3.65	5.24	49.13	4	−89.55	4.64	0.03
BMS_A	**NA**	–	**0.00**	**3.57**	**5.54**	**51.45**	**4**	**−94.19**	**0.00**	**0.31**
BMS_B	NA	–	0.00	3.63	4.60	49.30	4	−89.88	4.31	0.04
BMS_C	NA	–	0.00	3.66	4.01	49.66	4	−90.61	3.58	0.05

D. AEI thoracic

Model	α	ln(2)/α	σ^2	Θ_A	Θ	lnL	*k*	AICc	ΔAICc	AICcW
BM1	NA	–	0.00	6.92	–	30.19	2	−56.17	5.43	0.03
OU1	0.03	23.70	0.00	6.95	–	30.94	3	−55.46	6.13	0.02
OUM_A	0.06	11.86	0.00	6.60	10.00	34.66	4	−60.60	0.99	0.24
OUM_B	0.05	12.93	0.00	6.79	10.29	33.23	4	−57.75	3.84	0.06
OUM_C	0.04	15.76	0.00	6.92	16.09	33.47	4	−58.23	3.36	0.07
BMS_A	**NA**	**–**	**0.00**	**6.68**	**12.21**	**35.15**	**4**	**−61.59**	**0.00**	**0.39**
BMS_B	NA	–	0.00	6.79	12.81	34.21	4	−59.71	1.88	0.15
BMS_C	NA	–	0.00	6.88	26.08	33.12	4	−57.53	4.06	0.05

(continued)

Table 1. Continued.

E. AEI lumbar

Model	α	ln(2)/α	σ^2	Θ_A	Θ	lnL	*k*	AICc	ΔAICc	AICcW
BM1	NA	–	0.00	3.79	–	12.06	2	−19.92	5.21	0.03
OU1	0.00	–	0.00	3.79	–	12.06	3	−17.71	7.42	0.01
OUM_A	0.00	NA	0.00	3.57	10.28	16.34	4	−23.96	1.17	0.20
OUM_B	0.00	NA	0.00	3.71	7.97	13.56	4	−18.41	6.72	0.01
OUM_C	0.01	65.45	0.00	3.76	27.85	15.92	4	−23.12	2.01	0.13
BMS_A	NA	–	0.00	3.58	10.13	16.52	4	−24.33	0.80	0.24
BMS_B	NA	–	0.00	3.71	8.03	13.61	4	−18.51	6.62	0.01
BMS_C	**NA**	**–**	**0.00**	**3.77**	**22.96**	**16.92**	**4**	**−25.13**	**0.00**	**0.36**

F. AEI sacral

Model	α	ln(2)/α	σ^2	Θ_A	Θ	lnL	*k*	AICc	ΔAICc	AICcW
BM1	NA	–	0.00	1.53	–	33.42	2	−62.63	2.83	0.13
OU1	0.00	NA	0.00	1.53	–	33.42	3	−60.42	5.04	0.04
OUM_A	0.00	NA	0.00	1.49	2.50	35.83	4	−62.95	2.51	0.15
OUM_B	0.00	NA	0.00	1.52	2.04	33.94	4	−59.17	6.29	0.02
OUM_C	0.00	NA	0.00	1.53	3.56	34.68	4	−60.64	4.82	0.05
BMS_A	**NA**	**–**	**0.00**	**1.49**	**2.43**	**37.09**	**4**	**−65.46**	**0.00**	**0.53**
BMS_B	NA	–	0.00	1.52	2.02	34.05	4	−59.39	6.06	0.03
BMS_C	NA	–	0.00	1.53	3.56	34.68	4	−60.64	4.82	0.05

Optima have been converted back to raw values from ln transformed values. Rows in bold represent model with the highest AICcW scores.

appropriate by generating 1000 parametric bootstraps and determining AICcW for BMS at alpha = 0.05. The observed AICcW is far larger than this value, suggesting we can be confident in the selection of a BMS model here.

2-peak OUM and BMS models were also the best-fitting models for all morphological components underlying head-body ER (Table 1). These 2-peak models suggest that the mustelid subclade consisting of Helictidinae, Guloninae, Ictonychinae, Mustelinae, and Lutrinae exhibited larger trait optima in elongation of the cervical (OUM_A/BMS_A; combined AICcW = 0.58), thoracic (OUM_A/BMS_A; combined AICcW = 0.63), and sacral (OUM_A/BMS_A; AICcW = 0.68) regions. We found that accounting for the variation in the number of vertebrae did not affect inference of evolutionary transitions in the thoracic region as the best model was the BMS_A model (AICcW = 0.38; Table S2). We found that a 2-peak model for head ER (OUM_C; AICcW = 0.97) and lumbar region (BMS_C; AICcW = 0.36) supported a transition toward more elongate heads and more elongate lumbar vertebrae in musteline weasels and polecats only. However, the best-supported model for the lumbar region moved from the BMS_C model to the BMS_A model (AICcW = 0.33) when accounting for the variation in the number of lumbar vertebrae (Table S2).

In our analysis of regime transition in body size evolution, we found that a 2-peak BMS model (BMS_A) was the best model (AICcW = 0.90; Table 2). This model implies rapid evolution toward smaller size (Θ_A = 75.41; $\Theta_{mustelid}$ = 30.98) along the branch leading to a clade comprised of Helictidinae, Guloninae, Ictonychinae, Mustelinae, and Lutrinae and a subsequent return to BM like dynamics in the crown group.

Our model selection showed strong support for 2-peak BMS models (BMS_B) in our analyses of size-corrected forelimb (AICcW = 0.73) and hindlimb (AICcW = 0.74) lengths (Table 2). This indicates that a mustelid subclade consisting of the most recent common ancestors of Ictonychinae, Mustelinae, and Lutrinae evolved toward relatively shorter forelimbs ($\Theta_{mustelid}$ = 0.60) and hindlimbs ($\Theta_{mustelid}$ = 0.66) compared to the rest of the musteloid clade (forelimb Θ_A = 1.02 and hindlimb Θ_A = 1.00).

PREDICTION 2: TRANSITIONS IN BODY SHAPE ARE ACCOMPANIED BY TRANSITIONS IN BODY SIZE AND LIMB REDUCTION

We found a negative relationship between body size and head-body ER (λ = 0.354; $P < 0.001$), suggesting that head-body

Table 2. Parameter estimates and model fits of (A) body size, (B) forelimb length residuals, and (C) hindlimb length residuals.

A. Body size

Model	α	ln(2)/α	σ^2	Θ_A	Θ	lnL	*k*	AICc	ΔAICc	AICcW
BM1	NA	–	0.01	71.74	–	−10.93	2	26.06	15.48	0.00
OU1	0.02	44.57	0.01	71.23	–	−10.75	3	27.92	17.34	0.00
OUM_A	0.02	44.39	0.01	75.22	35.81	−9.41	4	27.53	16.95	0.00
OUM_B	0.02	33.27	0.01	72.72	40.02	−10.08	4	28.87	18.29	0.00
OUM_C	0.05	13.69	0.01	71.39	15.06	−8.97	4	26.65	16.07	0.00
BMS_A	NA	–	0.00	75.41	30.98	−0.93	4	10.58	0.00	0.90
BMS_B	NA	–	0.00	73.47	31.80	−3.20	4	15.12	4.54	0.09
BMS_C	NA	–	0.01	72.60	6.80	−8.27	4	25.26	14.68	0.00

B. forelimb length residuals

Model	α	ln(2)/α	σ^2	Θ_A	Θ	lnL	*k*	AICc	ΔAICc	AICcW
BM1	NA	–	0.00	1.00	–	58.37	2	−112.52	11.84	0.00
OU1	0.01	59.40	0.00	1.00	–	58.57	3	−110.72	13.64	0.00
OUM_A	0.03	21.21	0.00	1.01	0.78	60.27	4	−111.82	12.54	0.00
OUM_B	0.07	9.99	0.00	1.00	0.67	62.24	4	−115.76	8.60	0.01
OUM_C	0.01	59.90	0.00	1.00	0.88	58.63	4	−108.55	15.81	0.00
BMS_A	NA	–	0.00	1.02	0.76	65.49	4	−122.27	2.09	0.26
BMS_B	NA	–	0.00	1.02	0.60	66.54	4	−124.36	0.00	0.73
BMS_C	NA	–	0.00	1.00	0.87	58.44	4	−108.17	16.19	0.00

C. hindlimb length residuals

Model	α	ln(2)/α	σ^2	Θ_A	Θ	lnL	*k*	AICc	ΔAICc	AICcW
BM1	NA	–	0.00	1.00	–	60.02	2	−115.83	5.83	0.04
OU1	0.01	57.72	0.00	1.00	–	60.24	3	−114.06	7.60	0.02
OUM_A	0.02	37.10	0.00	1.01	0.88	60.64	4	−112.57	9.09	0.01
OUM_B	0.04	18.52	0.00	1.01	0.71	62.67	4	−116.62	5.04	0.06
OUM_C	0.01	59.74	0.00	1.00	0.89	60.30	4	−111.89	9.77	0.01
BMS_A	NA	–	0.00	1.01	0.89	63.42	4	−118.12	3.54	0.13
BMS_B	NA	–	0.00	1.01	0.66	65.19	4	−121.66	0.00	0.74
BMS_C	NA	–	0.00	1.00	0.91	60.86	4	−113.01	8.65	0.01

Optima have been converted back to raw values from ln transformed values. Rows in bold represent model with the highest AICcW scores.

elongation is associated with decreases in body size across musteloids (Fig. 4A). We did not find a significant relationship between size-corrected forelimb lengths and size-corrected head-body ER ($\lambda = 0.96$; $P = 0.088$) or between size-corrected hindlimb length and size-corrected head-body ER ($\lambda = 0.97$; $P = 0.438$). Scatter plots between body size, size-corrected head-body ER, and size-corrected limb lengths (Fig. 4) reveals that the sea otter (*Enhydra lutris*) is an outlier, exhibiting relatively short limbs for its body size and shape. The sea otter, the largest living musteloid, diverged from other otters 6 mya and exhibits several unique adaptations to its durophagous, marine lifestyle (Riedman and Estes 1990). Repeating the PGLS with the sea otter excluded results in a significant negative relationship between size-corrected forelimb lengths and size-corrected head-body ER ($\lambda = 0.95$; $P = 0.003$; Fig. 4B). The relationship between size-corrected hindlimb lengths and size-corrected head-body ER remains not significantly different ($\lambda = 0.97$; $P = 0.141$; Fig. 4C).

Discussion

Our study clearly shows that body elongation in a clade of mammals has converged on a suite of traits commonly observed in ectothermic vertebrate lineages: smaller, elongate body plans with reduced limbs. While mustelids are an additional example to the vertebrate corollary of limb reduction and increased body elongation (Fig. 4), we also found that the evolutionary trend for forelimb reduction prior to the reduction of hindlimbs as observed in

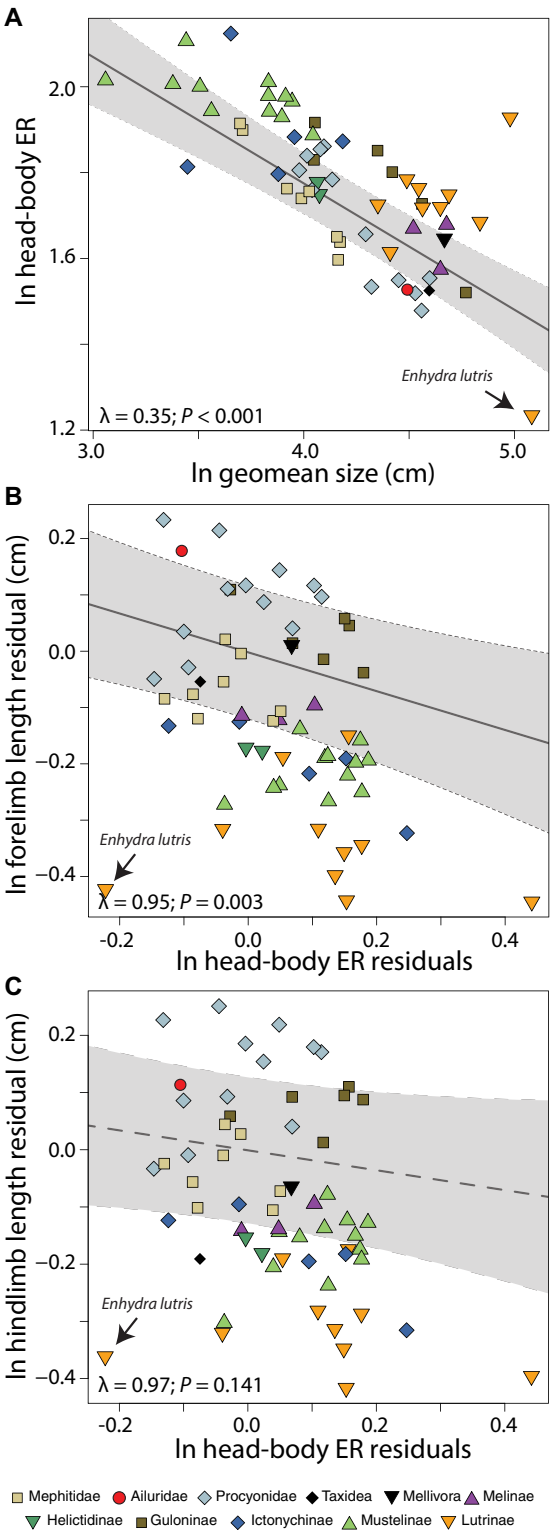

Figure 4. PGLS regressions of (A) ln geometric mean (body size) versus ln head-body ER (body shape), (B) ln head-body ER residuals versus ln forelimb length residuals, and (C) ln head-body ER residuals versus ln hindlimb length residuals. Head-body ER and limb length residuals were extracted from the residuals of each trait against the geometric mean (body size). Shaded polygons indicate the 95% confidence intervals.

multiple elongate lineages (Gans 1975; Wiens and Slingluff 2001; Brandley et al. 2008; Morinaga and Bergmann 2017) applies to mammals. These results suggest that the evolution of an elongate body plan is not constrained to ectothermic vertebrate clades, and traits associated with elongation of the body are fairly consistent across all vertebrates regardless of thermoregulatory process. The evolution of extreme body elongation in many ectothermic vertebrates is often associated with the evolution of innovative locomotor and foraging behaviors and performances that may lead to exploitation of novel resources (Webb 1982; Gans 1983; Brainerd and Patek 1998; Bergmann and Irschick 2009; Mehta et al. 2010). Whether the evolution of body shapes across all mammals is also associated with similar functional innovations remains to be tested. Furthermore, many elongate ectotherms also exhibit complete evolutionary loss of limbs (Gans 1975; Wiens and Slingluff 2001; Brandley et al. 2008; Morinaga and Bergmann 2017); the functional constraints that prevent terrestrial mammals from complete limb loss also requires additional investigation.

Because modifications away from these fixed vertebral numbers in mammals are rare, phylogenetically isolated events (Hautier and Weisbecker 2010; Varela-Lasheras et al. 2011; Buchholtz 2014), the evolution of more elongate body plans in mammals can likely only occur by reducing body depth, elongating the head, or increasing body length by lengthening vertebrae of one or more vertebral regions rather than increasing the number of vertebrae as found in ectothermic vertebrates. Most mustelid clades appear to elongate through elongation of the cervical, thoracic, and sacral regions of the vertebral column (Table 1). Weasels and polecats (subfamily Mustelinae) further elongated through elongation of the head and lumbar vertebrae (Table 1). However, musteline weasels and polecats also exhibit six lumbar vertebrae whereas most other musteloids exhibit four to five lumbar vertebrae (Narita and Kuratani 2005; this study). The extra lumbar vertebrae contribute to the overall elongation of the lumbar region and frees the constraints of ribs, which further facilitates dorsoventral flexibility and maneuverability during locomotion (Boszczyk et al. 2001). Increased spinal flexion allows musteline weasels and polecats to exhibit half-bound or bound gaits straight from walking without trotting, an unusual gait transition compared to other mammals (Williams 1983b) and increases their stride lengths and locomotor speed (Williams 1983b). Increased vertebral flexibility also aids in killing prey by allowing mustelines to wrap around prey with their elongate bodies to gain more mechanical leverage for the killing bite (Heidt 1972; King and Powell 2006).

INFLUENCES OF BODY SHAPE ON MUSTELOID DIVERSIFICATION AND DISPARITY

Our data showing transitions to a novel body shape within musteloids correspond with recent analyses of lineage diversification and evolutionary rates of body size. First, decoupling

of diversification processes just after the Mid-Miocene Climate transition occurred along the branch leading toward the mustelid crown clades Helictidinae, Guloninae, Ictonychinae, Mustelinae, and Lutrinae (Fig. 1) and resulted in a clade carrying capacity nearly twice as high as the remaining musteloid clade. Second, rates of body length evolution decoupled from body mass were consistent with an early-burst pattern within this mustelid subclade (Law et al. 2018). Together, transitions in body shape, decoupled length and mass relationships as well as increased carrying capacity provide evidence that the evolution of novel body plans enabled mustelids to exploit the new open grassland, steppe, and taiga forest habitats and their associated small rodent and lagomorph faunas during the continual cooling and drying of the Late Miocene to Pliocene (Brown et al. 1972; Gliwicz 1988; King 1989). These findings indicate that 14 to 5 MYA was a critical time in mustelid morphological evolution. Yet, few studies have examined the phylogenetic relationships among extinct mustelids from this period. Qualitative examination of the musteloid fossil record supports hypotheses relating elongate body shapes to ecological opportunity. Small extinct neomustelids such as †*Cernictis*, †*Trigonictis*, and †*Sminthosinis,* which are morphologically similar to extant mustelines and ictonychines (Baskin 1998), became abundant during the late Miocene and Pliocene of North America and Eurasia (Ruez 2016), and replaced stem mustelids ("paleomustelids") lineages (Law et al. 2018). There is some evidence that paleomustelids or musteloids may have used rodent burrows (e.g., a specimen of the musteloid †*Zodiolestes* has been recovered from an extinct beaver †*Palaeocastor* burrow) but it is unclear whether this represents opportunistic use of the burrow as a shelter or evidence of specialist predation (Martin and Bennett 1977). Future work incorporating morphometric data from extinct musteloid taxa in a robust phylogeny would fill a critical gap in the evolutionary history of this clade and provide a more robust framework for testing hypotheses about the evolution of body shape from a paleobiological perspective.

Elongate bodies facilitate undulatory locomotion in many squamate clades (Gans 1975; Skinner et al. 2008; Bergmann and Irschick 2009), but some researchers have begun to view reduced limbs as an equally important adaptation in aiding this form of locomotion (Brandley et al. 2008). Moving through tunnels is one of the primary physical challenges for limbed animals, as postural adaptations are needed to accommodate the body and limb swing in a constrained environment. Although musteline weasels and polecats are not burrowers themselves and have not been observed to perform undulatory locomotion, they nevertheless exploit the burrows of their prey (e.g., Heidt 1972; Erlinge 1981; Clark et al. 1986; King 1989). Kinematic trials with domestic ferrets (*Mustela putorius furo*) reveal that their elongate bodies and short-limbs enable them to reduce their back heights by 34% and hip heights by 23.5% when traveling through tunnels (Horner et al. 2016). This allows ferrets to maintain the same gait as when traveling above ground (Horner and Biknevicius 2010) and facilitates more efficient cost of transport compared to other similar sized mammals (Horner et al. 2016). Ictonychines, particularly the African striped weasel (*Poecilogale albinucha*), also exhibit elongate morphologies. Like mustelines, most ictonychines specialize on small rodents in grassland habitats and frequently chase prey in burrows and crevices (Larivière 2001). Therefore, convergence toward similar dietary specializations, predatory behaviors, and elongate body shapes with musteline weasels and polecats provide additional evidence that increased body elongation facilitates resource use.

Martens (*Martes* spp.—Guloninae) also transitioned towards more elongate body shapes with similar head-body ERs to musteline weasels and polecats. Similarly, weasels, polecats, and martens hunt for rodents, lagomorphs, and other small vertebrates and may use their elongate bodies to maneuver through burrows and tunnels (Clark et al. 1987; Wilson et al. 2009). Unlike weasels and polecats, martens exhibit relatively long limbs despite their elongate body plans (Fig. 3; Fig. 4). Many martens are semi-arboreal (Clark et al. 1987; Posłuszny et al. 2007), and relatively longer limbs may be advantageous in maneuvering rapidly in trees. A semi-arboreal predatory lifestyle may also favor a body plan that redistributes mass over a longer area for enhanced balance and a lighter load at any one point along branches. Semi-arboreal feliform carnivorans such as genets and linsangs, have also been qualitatively described as elongate, and the potential advantages of an elongate body plan for arboreal carnivory and quantification of the body shapes of other arboreal carnivorans requires additional work.

Contrary to functional and phylogenetic expectations, we found that otters exhibit some of the lowest head-body ERs within Mustelidae. Otters are semi-aquatic mustelids that form the sister group to the elongate musteline weasels and polecats. Fully aquatic mammals are well-streamlined, with fineness ratios (body length to thickness ratio) within the optimal range of 3.3–7.0 (Fish 1993) resulting in reduced total body drag (Fish 1996). However, becoming too elongate results in body dimensions outside of the optimal range of fineness ratios and reduces swimming efficiency (Mises 1945; Webb 1975; Fish 1993). Indeed, otter species nearing the optimal fineness ratio exhibit greater swimming efficiency compared to other mammals of similar sizes (Williams 1989; Fish 1994). However, despite their less elongate bodies, otters exhibit the shortest limb lengths for their body size (Fig. 3H, I). Reduction of the limbs along with interdigital webbing contributes to streamlining of the body and therefore reduces drag by shifting the swimming gait from paddling or drag-based propulsion to undulatory propulsion (Williams 1989; Fish 1993, 1994, 1996). Additionally, some otter species exhibit long, paddle-like tails that may further increase swimming efficiency. These longer

tails may also have made the silhouettes of otters appear more elongate than they actually are. Alternatively, otters may have secondarily evolved shortened axial skeletons to increase swimming efficiency. Semi-aquatic American minks (*Mustela vison*, subfamily Mustelinae) exhibit a fineness ratio that surpasses the optimal range (Williams 1983a) and approaches higher ends of head-body ER values in our dataset. Therefore, American minks, despite being active foragers in the water (Larivière 1999), are too elongate to perform more efficient forms of fast swimming locomotion, and instead are constrained to use inefficient drag-based paddling for propulsion (Williams 1983a, 1989; Fish 1993, 1994, 1996). A more detailed examination of the sparse lutrine fossil record would help shed light on this interesting transition.

An elongate body, however, presents metabolic challenges by increasing an animal's surface area to volume ratio, which, in turn increases heat loss resulting in elevated metabolic rates (Brown et al. 1972; Iversen 1972; Williams 1983a). Unsurprisingly, mustelids exhibit higher metabolic rates compared to other similar sized mammals (Brown et al. 1972; Iversen 1972; Williams 1983a). The thermoregulatory challenges imposed by an elongate body may be partially offset by behavioral innovations. Some musteline weasels and polecats line their burrows with the fur and feathers of their prey to presumably keep warm during cooler temperatures (Polderboer et al. 1941; Novikov 1956). Furthermore, most musteline weasels and polecats exhibit caching behavior, allowing individuals to survive in their burrows for several days without the need to hunt for more food in the open (Oksanen et al. 1985; Jedrzejewska and Jedrzejewski 1989; King and Powell 2006). On the other hand, otters are semi-aquatic but lack blubber and therefore encounter rapid heat loss when immersed in water despite their fur (Costa and Kooyman 1982). The energetic cost of swimming is also high, resulting in elevated field metabolic rates during aquatic locomotion (Morrison et al. 1974; Costa and Kooyman 1984; Pfeiffer and Culik 1998; Borgwardt and Culik 1999; Dekar et al. 2010; Thometz et al. 2014). Consequently, a less elongate body and relatively shorter limbs in otters may serve as a secondary advantage in reducing heat loss.

Conclusion

Morphological disparity can play an influential role in species diversification. Here, we examined the evolution of body shape in musteloids. Previous work revealed musteloids exhibit decoupled diversification dynamics driven by increased clade carrying capacity in the branches leading to a subclade of mustelids and a lack of correspondence in body length and body mass evolutionary rates within the decoupled mustelid subclade (Law et al. 2018). We show that despite constraints in vertebral numbers, evolutionary transitions to extreme body shapes are possible in mammals and provide valuable insights into how seemingly subtle changes in morphology can lead to the occupation of new adaptive zones. These findings together indicate that the transition to body elongation may be an important morphological innovation that contributed to the diversification of some mustelids, particularly musteline weasels and polecats. We found that the mustelid crown clades (Helictidinae, Guloninae, Ictonychinae, Lutrinae, and Mustelinae) exhibited evolutionary transitions toward more elongate body shape optima via elongation of cervical, thoracic, and sacral regions, smaller body sizes, and reduced limb lengths. Musteline weasels and polecats became even more elongate through elongation of the cranium and lumbar region. We further found body elongation exhibited negative relationships with body size and forelimb length but not hindlimb length, suggesting that more elongate species are smaller and exhibit relatively shorter forelimbs. This relationship between body elongation and forelimb length follows the major trend exhibited by other vertebrates, suggesting that an elongate body with reduced forelimbs is advantageous in many vertebrate clades, particularly in lineages that exploit subterranean habitats (Gans 1975; Wiens et al. 2006).

AUTHOR CONTRIBUTIONS

C.J.L., G.J.S., and R.S.M. conceived the study. C.J.L. collected the body shape data, performed the macroevolutionary analyses, and drafted the manuscript. R.S.M. helped collect body shape data. G.J.S. provided crucial insights on macroevolutionary methods. R.S.M. and G.J.S. helped develop the approach and revised the manuscript. All authors read and approved the final manuscript.

ACKNOWLEDGMENTS

We are grateful for the access to specimens provided by museum collection managers and curators including Eleanor Hoeger, Brian O'Toole, and Eileen Westwig of AMNH; Moe Flannery of CAS; Adam Ferguson, Bruce Patterson, and Lauren Smith of FMNH; Jonathan Dunnum of MSB; Chris Conroy and Jim Patton of MVZ; Darrin Lunde and John Ososky of NMNH; and Jim Dines of LACM. We also thank the remaining members of C.J.L.'s PhD committee (Kathleen Kay, Tim Tinker, and Terrie Williams), Vikram Baliga, Associate Editor Jessica Light, Joshua Samuels, Roger Powell, and five anonymous reviewers for constructive feedback. This manuscript fulfilled partial requirements for a Ph.D degree at the University of California, Santa Cruz. This work was supported by a James Patton Award through the American Society of Mammalogists, an AMNH Collection Study Grant, a Society of Integrative and Comparative Biology Fellowship Graduate Student Travel, a Field Museum Visiting Scholarship, and a National Science Foundation Graduate Research Fellowship and Doctoral Dissertation Improvement Grant (C.J.L.).

CONFLICT OF INTERESTS

The authors have no competing interests.

DATA ARCHIVING

All datasets and scripts used in this study as well as additional tables have been uploaded onto dryad.
The doi for data is https://doi.org/10.5061/dryad.m55q9p0.

LITERATURE CITED

Arnold, P., E. Amson, and M. S. Fischer. 2017. Differential scaling patterns of vertebrae and the evolution of neck length in mammals. Evolution 85:2706–2713.

Baskin, J. A. 1998. Mustelidae. Pp. 152–173 *in* C. M. Janis, K. M. Scott, and L. L. Jacobs, eds. Evolution of tertiary mammals of North America: Terrestrial carnivores, ungulates, and ungulatelike mammals. Cambridge Univ. Press, United Kingdom.

Beaulieu, J. M., D.-C. Jhwueng, C. Boettiger, and B. C. O'Meara. 2012. Modeling stabilizing selection: expanding the Ornstein-Uhlenbeck model of adaptive evolution. Evolution 66:2369–2383.

Bergmann, P. J., and D. J. Irschick. 2009. Alternate pathways of body shape evolution translate into common patterns of locomotor evolution in two clades of lizards. Evolution 64:1569–1582.

———. 2012. Vertebral evolution and the diversification of squamate reptiles. Evolution 66:1044–1058.

Borgwardt, N., and B. M. Culik. 1999. Asian small-clawed otters (*Amblonyx cinerea*): resting and swimming metabolic rates. J. Comp. Physiol. B Biochem. Syst. Environ. Physiol. 169:100–106.

Boszczyk, B. M., A. A. Boszczyk, and R. Putz. 2001. Comparative and functional anatomy of the mammalian lumbar spine. Anatomical Record 264:157–168.

Brainerd, E. L., and S. N. Patek. 1998. Vertebral column morphology, C-start curvature, and the evolution of mechanical defenses in tetraodontiform fishes. Copeia 1998:971–984.

Brandley, M. C., J. P. Huelsenbeck, and J. J. Wiens. 2008. Rates and patterns in the evolution of snake-like body form in squamate reptiles: evidence for repeated re-evolution of lost digits and long-term persistence of intermediate body forms. Evolution 62:2042–2064.

Buchholtz, E. A. 2001. Vertebral osteology and swimming style in living and fossil whales (Order: Cetacea). J. Zool. 253:175–190.

———. 2014. Crossing the frontier: a hypothesis for the origins of meristic constraint in mammalian axial patterning. Zoology 117:64–69.

Buchholtz, E. A., and S. A. Schur. 2004. Vertebral osteology in Delphinidae (Cetacea). Zool. J. Linn. Soc. 140:383–401.

Butler, M. A., and A. A. King. 2004. Phylogenetic comparative analysis: a modeling approach for adaptive evolution. Am. Nat. 164:683–695.

Clark, T. W., E. Anderson, C. Douglas, and M. Strickland. 1987. *Martes americana*. Mammalian Species 1–8. Mammalian species.

Clark, T. W., L. Richardson, S. C. Forrest, and D. E. Casey. 1986. Descriptive ethology and activity patterns of black-footed ferrets. Great Basin Nat. Memoirs 8:115–134.

Claverie, T., and P. C. Wainwright. 2014. A morphospace for reef fishes: elongation is the dominant axis of body shape evolution. PLoS ONE 9:e112732.

Collar, D. C., C. M. Reynaga, A. B. Ward, and R. S. Mehta. 2013. A revised metric for quantifying body shape in vertebrates. Zoology 116:246–257.

Collar, D. C., M. Quintero, B. Buttler, A. B. Ward, and R. S. Mehta. 2016. Body shape transformation along a shared axis of anatomical evolution in labyrinth fishes (Anabantoidei). Evolution 70:555–567.

Costa, D. P., and G. L. Kooyman. 1984. Contribution of specific dynamic action to heat-balance and thermoregulation in the sea otter *Enhydra lutris*. Physiol. Zool. 57:199–203.

Costa, D. P., and G. L. Kooyman. 1982. Oxygen consumption, thermoregulation, and the effect of fur oiling and washing on the sea otter, *Enhydra lutris*. Can. J. Zool. 60:2761–2767.

Cundall, D., and H. W. Greene. 2000. Feeding in Snakes. Pp. 293–333 *in* K. Schwenk, ed. Feeding: Form, function and evolution in tetrapod vertebrates. Academic Press, San Diego, CA.

Dekar, M. P., D. D. Magoulick, and J. Beringer. 2010. Bioenergetics assessment of fish and crayfish consumption by river otter (*Lontra canadensis*): integrating prey availability, diet, and field metabolic rate. Can. J. Fish. Aquat. Sci. 67:1439–1448.

Diluzio, A. R., V. B. Baliga, B. A. Higgins, and R. S. Mehta. 2017. Effects of prey characteristics on the feeding behaviors of an apex marine predator, the California moray (*Gymnothorax mordax*). Zoology 122:80–89.

Edwards, E. J., C. P. Osborne, C. A. E. Strömberg, S. A. Smith, and C. G. Consortium. 2010. The origins of C4 grasslands: integrating evolutionary and ecosystem science. Science 328:587–591.

Erlinge, S. 1981. Food preference, optimal diet and reproductive output in stoats *Mustela erminea* in Sweden. Oikos 36:303–315.

Fabre, P.-H., L. Hautier, D. Dimitrov, and E. J. P. Douzery. 2012. A glimpse on the pattern of rodent diversification: a phylogenetic approach. BMC Evol. Biol. 12:88.

Finarelli, J. A., and C. Badgley. 2010. Diversity dynamics of Miocene mammals in relation to the history of tectonism and climate. Proc. R Soc. B 277:2721–2726.

Fish, F. E. 1993. Influence of hydrodynamic-design and propulsive mode on mammalian swimming energetics. Austral. J. Zool. 42:79–101.

———. 1994. Association of propulsive swimming mode with behavior in river otters (*Lutra canadensis*). J. Mammal. 75:989–997.

———. 1996. Transitions from drag-based to lift-based propulsion in mammalian swimming. Am. Zool. 36:628–641.

Fish, F. E., L. E. Howle, and M. M. Murray. 2008. Hydrodynamic flow control in marine mammals. Integr. Comp. Biol. 48:788–800.

Gans, C. 1975. Tetrapod limblessness: evolution and functional corollaries. Amer. Zool. 15:455–467.

———. 1983. Snake feeding strategies and adaptations—conclusion and prognosis. Am. Zool. 23:455–460.

Gavryushkina, A., D. Welch, T. Stadler, and A. J. Drummond. 2014. Bayesian inference of sampled ancestor trees for epidemiology and fossil calibration. PLoS Comput. Biol. 10:e1003919.

Gliwicz, J. 1988. Sexual dimorphism in small mustelids: body diameter limitation. Oikos 53:411.

Gray, J. E. 1865. Revision of the genera and species of Mustelidae contained in the British Museum. J. Zool. 33:100–154.

Griffith, E. 1827. The Animal Kingdom arranged in conformity with its organization with additional descriptions of all the species hitherto named, and of many not before noticed Volume the fifth. G.B. Whittaker, London.

Hansen, T. F. 1997. Stabilizing selection and the comparative analysis of adaptation. Evolution 51:1341–1351.

Hautier, L., and V. Weisbecker. 2010. Skeletal development in sloths and the evolution of mammalian vertebral patterning. Proc. Natl. Acad. Sci. USA 107:18903–18908.

Heath, T. A., J. P. Huelsenbeck, and T. Stadler. 2014. The fossilized birth-death process for coherent calibration of divergence-time estimates. Proc. Natl. Acad. Sci. USA 111:E2957–E2966.

Heidt, G. A. 1972. Anatomical and behavioral aspects of killing and feeding by the least weasel, *Mustela nivalis* L. Arkansas Academy of Science Proceedings.

Holmes, T., and R. A. Powell. 1994. Morphology, ecology and the evolution of sexual dimorphism in North American *Martes*. Pp. 72–84 *in* S. W. Buskirk, A. S. Harestad, M. G. Raphael, and R. A. Powell, eds. Martens, sables and fishers biology and conservation. Ithaca, New York, USA.

Horner, A. M., and A. R. Biknevicius. 2010. A comparison of epigean and subterranean locomotion in the domestic ferret (*Mustela putorius furo*: Mustelidae: Carnivora). Zoology 113:189–197.

Horner, A. M., J. B. Hanna, and A. R. Biknevicius. 2016. Crouching to fit in: the energetic cost of locomotion in tunnels. J. Exp. Biol. 219:3420–3427.

Iversen, J. A. 1972. Basal energy metabolism of mustelids. J. Comp. Physiol. A 81:341–344.

J. H. Brown, Lasiewski, R. C., Brown, J. H., and R. C. Lasiewski. 1972. Metabolism of weasels: the cost of being long and thin. Ecology 53: 939–943.

Jedrzejewska, B., and W. Jedrzejewski. 1989. Seasonal surplus killing as hunting strategy of the weasel *Mustela nivalis*—test of a hypothesis. Acta Theriol. 34:347–359.

Jungers, W. L., A. B. Falsetti, and C. E. Wall. 1995. Shape, relative size, and size-adjustments in morphometrics. Am. J. Phys. Anthropol. 38: 137–161.

Kardong, K. V. 2014. Vertebrates: Comparative anatomy, function, evolution. McGraw-Hill Education, Boston.

King, C. M. 1989. The advantages and disadvantages of small size to weasels, *Mustela* Species. Pp. 302–334 *in* J. L. Gittleman, ed. Carnivore behavior, ecology, and evolution. Springer US, Boston, MA.

King, C. M., and R. A. Powell. 2006. Hunting behavior. Pp. 113–136 *in* C. M. King and R. A. Powell, eds. The natural history of weasels and stoats ecology, behavior, and management. Oxford Univ. Press, Oxford.

Koepfli, K.-P., K. A. Deere, G. J. Slater, C. Begg, K. Begg, L. Grassman, M. Lucherini, G. Veron, and R. K. Wayne. 2008. Multigene phylogeny of the Mustelidae: resolving relationships, tempCEo and biogeographic history of a mammalian adaptive radiation. BMC Biol. 6: 10.

Larivière, S. 1999. *Mustela vison*. Mamm. Species 1–9.

———. 2001. *Poecilogale albinucha*. Mamm. Species 681:1–4.

Law, C. J., and R. S. Mehta. 2018. Carnivory maintains cranial dimorphism between males and females: evidence for niche divergence in extant Musteloidea. Evolution 72:1950–1961.

Law, C. J., G. J. Slater, and R. S. Mehta. 2018. Lineage diversity and size disparity in Musteloidea: testing patterns of adaptive radiation using molecular and fossil-based methods. Syst. Biol. 67:127–144.

Lillywhite, H. B. 2014. How snakes work: Structure, function and behavior of the world's snakes. Oxford Univ. Press, Oxford.

Lindstedt, S. L., and M. S. Boyce. 1985. Seasonality, fasting endurance, and body size in mammals. Am. Nat. 125:873–878.

Martin, L. D., and D. K. Bennett. 1977. The burrows of the Miocene beaver *Palaeocastor*, western Nebraska, USA. Palaeogeogr. Palaeoclimatol. Palaeoecol. 22:173–193.

Mehta, R. S., A. B. Ward, M. E. Alfaro, and P. C. Wainwright. 2010. Elongation of the body in eels. Integr. Comp. Biol. 50:1091–1105.

Mehta, R. S., and P. C. Wainwright. 2007. Raptorial jaws in the throat help moray eels swallow large prey. Nature 449:79–82.

Miller, T. J. 1989. Feeding behavior of *Echidna nebulosa*, *Enchelycore pardalis*, and *Gymnomuraena zebra* (Teleostei: Muraenidae). Copeia 1989:662–672.

Mises, Von, R. 1945. Theory of flight. Courier Corporation, Massachusetts.

Morinaga, G., and P. J. Bergmann. 2017. Convergent body shapes have evolved via deterministic and historically contingent pathways in *Lerista* lizards. Biol. J. Linn. Soc. 121:858–875.

Morris, J. S., and D. R. Carrier. 2016. Sexual selection on skeletal shape in Carnivora. Evolution 70:767–780.

Morrison, P., M. Rosenmann, and J. A. Estes. 1974. Metabolism and thermoregulation in the sea otter. Physiol. Zool. 47:218–229.

Mosimann, J. E. 1970. Size allometry: size and shape variables with characterizations of the lognormal and generalized gamma distributions. J. Am. Stat. Assoc. 65:930–945.

Narita, Y., and S. Kuratani. 2005. Evolution of the vertebral formulae in mammals: a perspective on developmental constraints. J. Exp. Zool. 304B:91–106.

Novikov, G. A. 1956. Carnivorous mammals of the fauna of the USSR. Nauka Publishing House, Moscow-Leningrad, Soviet Union. pg. 283 (in Russian).

Oksanen, T., L. Oksanen, and S. D. Fretwell. 1985. Surplus killing in the hunting strategy of small predators. Am. Nat. 126:328–346.

Pagel, M. 1999. Inferring the historical patterns of biological evolution. Nature 401:877–884.

Parra-Olea, G., and D. B. Wake. 2001. Extreme morphological and ecological homoplasy in tropical salamanders. Proc. Natl. Acad. Sci. USA 98:7888–7891.

Pfeiffer, P., and B. M. Culik. 1998. Energy metabolism of underwater swimming in river-otters (*Lutra lutra* L.). J. Comp. Physiol. B 168:143–148.

Polderboer, E. B., L. W. Kuhn, and G. O. Hendrickson. 1941. Winter and spring habits of weasels in central Iowa. J. Wildl. Manage. 5:115.

Polly, P. D., J. J. Head, and M. J. Cohn. 2001. Testing modularity and dissociation: the evolution of regional proportions in snakes. Pp. 305–335 *in* M. L. Zelditch, ed. Beyond heterochrony: The evolution of development. Wiley, Hoboken, New Jersey.

Posłuszny, M., M. Pilot, J. Goszczyński, and B. Gralak. 2007. Diet of sympatric pine marten (*Martes martes*) and stone marten (*Martes foina*) identified by genotyping of DNA from faeces. Ann. Zool. Fennici 44:269–284.

R Core Team. 2017. R: a language and environment for statistical computing. R Foundation for Statistical Computing, Vienna, Austria.

Revell, L. J. 2010. Phylogenetic signal and linear regression on species data. Methods Ecol. Evol. 1:319–329.

———. 2011. phytools: an R package for phylogenetic comparative biology (and other things). Methods Ecol. Evol. 3:217–223.

Richardson, M. K., S. P. Allen, G. M. Wright, A. Raynaud, and J. Hanken. 1998. Somite number and vertebrate evolution. Development 125: 151–160.

Riedman, M., and J. A. Estes. 1990. The sea otter (*Enhydra lutris*): behavior, ecology, and natural history. Biol. Rep. 90:1–117.

Ruez, D. 2016. Stratigraphic changes in the pliocene carnivoran assemblage from Hagerman Fossil Beds National Monument, Idaho. Geosciences 6:15–9.

Samuels, J. X., and S. S. B. Hopkins. 2017. The impacts of Cenozoic climate and habitat changes on small mammal diversity of North America. Glob. Planet. Change 149:36–52.

Sato, J. J., M. Wolsan, F. J. Prevosti, G. D'Elía, C. Begg, K. Begg, T. Hosoda, K. L. Campbell, and H. Suzuki. 2012. Evolutionary and biogeographic history of weasel-like carnivorans (Musteloidea). Mol. Biol. Evol. 63:745–757.

Scholander, P. F., V. Walters, and R. Hock. 1950. Body insulation of some arctic and tropical mammals and birds. Biol. Bull. 99:225–236.

Sharpe, S. S., S. A. Koehler, R. M. Kuckuk, M. Serrano, P. A. Vela, J. Mendelson, and D. I. Goldman. 2015. Locomotor benefits of being a slender and slick sand-swimmer. J. Exp. Biol. 218:440–450.

Shaw, G. 1800. General zoology or systematic natural history, vol. I. Part 1. Mammalia. Thomas Davison, London.

Skinner, A., M. S. Lee, and M. N. Hutchinson. 2008. Rapid and repeated limb loss in a clade of scincid lizards. BMC Evol. Biol. 8:310–9.

Strömberg, C. A. E. 2011. Evolution of grasses and grassland ecosystems. Annu. Rev. Earth Planet. Sci. 39:517–544.

Thomas, G. H., R. P. Freckleton, and T. Székely. 2006. Comparative analyses of the influence of developmental mode on phenotypic diversification rates in shorebirds. Proc. R Soc. B 273:1619–1624.

Thometz, N. M., M. T. Tinker, M. T. Tinker, M. Staedler, M. M. Staedler, K. A. Mayer, T. M. Williams, and T. M. Williams. 2014. Energetic demands of immature sea otters from birth to weaning: implications for maternal

costs, reproductive behavior and population-level trends. J. Exp. Biol. 217:2053–2061.

Tung Ho, L. S., and C. Ané. 2014. A linear-time algorithm for Gaussian and non-Gaussian trait evolution models. Syst. Biol. 63:397–408.

Varela-Lasheras, I., A. J. Bakker, S. D. van der Mije, J. A. Metz, J. van Alphen, and F. Galis. 2011. Breaking evolutionary and pleiotropic constraints in mammals: on sloths, manatees and homeotic mutations. EvoDevo 2: 1–27.

Ward, A. B., and E. L. Brainerd. 2007. Evolution of axial patterning in elongate fishes. Biol. J. Linn. Soc. 90:97–116.

Ward, A. B., and R. S. Mehta. 2010. Axial elongation in fishes: using morphological approaches to elucidate developmental mechanisms in studying body shape. Integr. Comp. Biol. 50:1106–1119.

Ward, A. B., and R. S. Mehta. 2014. Differential occupation of axial morphospace. Zoology 117:70–76.

Webb, P. W. 1975. Hydrodynamics and energetics of fish propulsion. Bull. Fish. Res. Board Can. 190:1–156.

———. 1982. Locomotor patterns in the evolution of actinopterygian fishes. Amer. Zool. 22:329–342.

Wiens, J. J., and J. L. Slingluff. 2001. How lizards turn into snakes: a phylogenetic analysis of body-form evolution in anguid lizards. Evolution 55:2303–2318.

Wiens, J. J., M. C. Brandley, and T. W. Reeder. 2006. Why does a trait evolve multiple times within a clade? Repeated evolution of snakelike body form in squamate reptiles. Evolution 60:123–141.

Williams, T. M. 1983a. Locomotion in the North American mink, a semi-aquatic mammal. I. Swimming energetics and body drag. J. Exp. Biol. 103:155–168.

———. 1983b. Locomotion in the North American mink, a semi-aquatic mammal. II. The effect of an elongate body on running energetics and gait patterns. J. Exp. Biol. 105:283–295.

———. 1989. Swimming by sea otters: adaptations for low energetic cost locomotion. J. Comp. Physiol. 164:815–824.

Wilson, D. E., R. A. Mittermeier, and R. A. Mittermeier. 2009. Handbook of the mammals of the world. Lynx Edicions, Spain.

Zachos, J. C., G. R. Dickens, and R. E. Zeebe. 2008. An early Cenozoic perspective on greenhouse warming and carbon-cycle dynamics. Nature 451:279–283.

Zielinski, W. J. 2000. Weasels and Martens—carnivores in Northern Latitudes. Pp. 95–118 *in* S. Halle and N. C. Stenseth, eds. Activity patterns in small mammals. Springer Berlin Heidelberg, Berlin, Heidelberg.

Associate Editor: J. Light
Handling Editor: M. Servedio

Supporting Information

Additional supporting information may be found online in the Supporting Information section at the end of the article.

Table S1. Catalog number of all specimens used in this study.
Table S2. Parameter estimates and model fits for the average aspect ratio of the (A) thoracic and (B) lumbar vertebrae.